

Measurement of CP violation and mixing in $B_s^0 \rightarrow J/\psi\phi$ in ATLAS

ICHEP 2020

Prague, Czech Republic

28 July to 6 August 2020

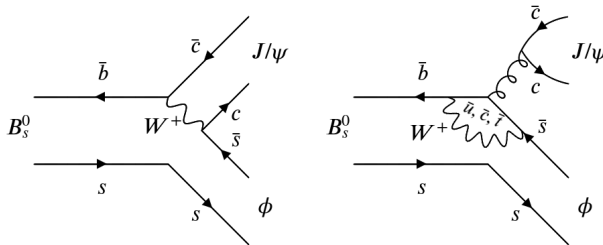
Tomáš Jakoubek on behalf of the ATLAS Collaboration

Weizmann Institute of Science

tomas.jakoubek@cern.ch

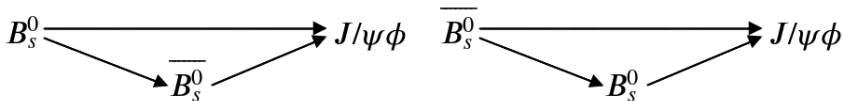
Introduction

- Decay $B_s^0 \rightarrow J/\psi \phi$ is expected to be sensitive to new physics contributions to CP violation.
- Neutral B_s^0 meson can oscillate into its antiparticle \overline{B}_s^0 (and vice versa).
- The oscillation frequency is characterized by the mass difference Δm_s of the heavy (B_H) and light (B_L) mass eigenstates.
- In the absence of CP violation, the B_H state would correspond to the CP -odd state and the B_L to the CP -even state.



Types of CP Violation

- **CP violation in decay** (or direct CP violation): decay amplitudes of mesons $M \rightarrow f$ and $\bar{M} \rightarrow \bar{f}$ are different.
- **CP violation in mixing** (or indirect CP violation): asymmetry in the particle antiparticle oscillations... In this case the CP eigenstates are not equivalent to the mass eigenstates.
- **CP violation in interference of mixing and decay** can only occur if M^0 and \bar{M}^0 decay into the same final state;
The common final state is reached via two different decay chains: $M^0 \rightarrow f$ and $M^0 \rightarrow \bar{M}^0 \rightarrow f$ (case of $B_s^0 \rightarrow J/\psi\phi$).



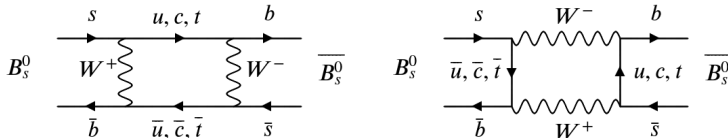
Motivation: New Physics

- CP violating phase is defined as the weak phase difference between the $B_s^0 - \overline{B}_s^0$ mixing amplitude and the $b \rightarrow c\bar{c}s$ decay amplitude.
- In the Standard Model (SM) it can be related to the CKM matrix [1]

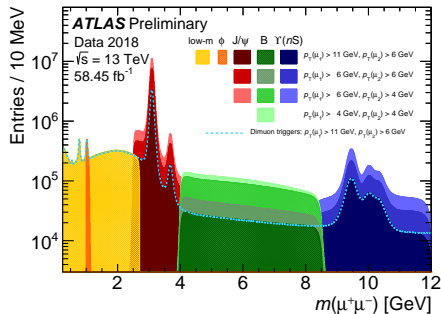
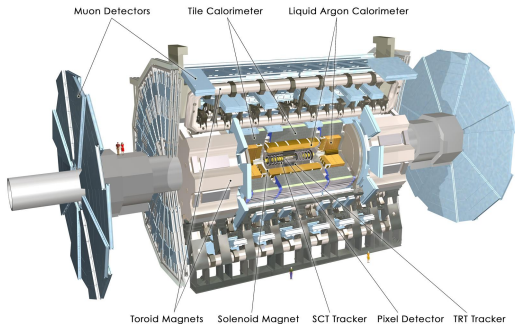
$$\phi_s \simeq -2\beta_s = -2 \arg \left(-\frac{V_{ts} V_{tb}^*}{V_{cs} V_{cb}^*} \right). \quad (1)$$

and then $\phi_s = -0.03696_{-0.00082}^{+0.00072}$ rad can be predicted [2].

- Any sizeable deviation from this value would be a sign of beyond SM physics.
- The New Physics processes could introduce additional contributions to the box diagrams describing the $B_s^0 - \overline{B}_s^0$ mixing.



The ATLAS Experiment



- **Muon Spectrometer:** triggering $|\eta| < 2.4$ and precision tracking $|\eta| < 2.7$.
- **Inner Detector:** Silicon Pixels and Strips with Transition Radiation Tracker, $p_T > 0.4$ GeV and $|\eta| < 2.5$,
- **NEW in Run2:** “Insertable B-Layer” (IBL) - additional inner-most pixel layer ($r = 33$ mm) and lower x/X_0 beam pipe,
- **resolution in $m(\mu^+\mu^-)$:** Around 50 MeV at J/ψ , 150 MeV at $\Upsilon(nS)$,
- **resolution in b -hadron proper decay time:** ~ 100 fs (30 % improvement with IBL).



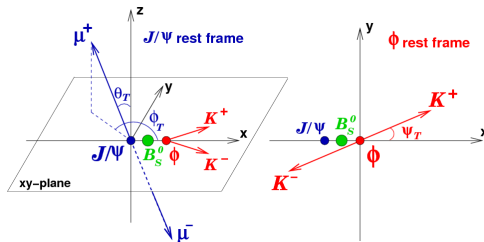
Used Data

- 4.9 fb^{-1} 7 TeV pp 2011 (untagged [5] + tagged [6]).
- 14.3 fb^{-1} 8 TeV pp 2012 (statistically combined with 7 TeV to full Run1 tagged analysis [7]).
- **NEW:** 80.5 fb^{-1} 13 TeV pp 2015-2017 (stat. comb. with Run1 [8]).
- Collected by trigger based on identification of $J/\psi \rightarrow \mu^+ \mu^-$ with $p_T(\mu)$ thresholds varying over run periods (but always low- p_T , 4 or 6 GeV).
- Two muon tracks and two tracks (no PID, but not muons).
- 4 tracks refitted to a common vertex.
- In case of multiple candidates, using only the best candidate in the event.
- Signal-background separation done completely by an unbinned maximum likelihood fit.



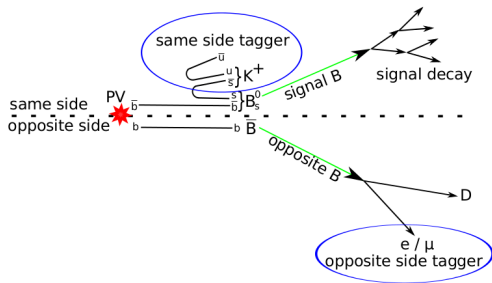
Angular Analysis

- $B_s^0 \rightarrow J/\psi\phi$ = pseudoscalar to vector-vector final state \rightarrow admixture of CP -odd ($L = 1$) and CP -even ($L = 0, 2$) states.
- Distinguishable through time-dependent angular analysis.
- Non-resonant S -wave decay $B_s^0 \rightarrow J/\psi K^+ K^-$ and $B_s^0 \rightarrow J/\psi f_0$ both contribute to the final state:
 - can't be identified in the measured data, but can significantly bias measurement of ϕ_s ,
 - thus they have to be included in the differential decay rate (due to interference with the signal decay) and treated by the fit.



Flavour Tagging

- Knowledge of the initial flavour can improve any CP violation measurement.
- At the LHC B -mesons are produced in the hadronization of $b\bar{b}$ pair.
- The majority of these pairs are produced either both in the forward or both in the backward direction of the detector.
- Self-tagging $B^\pm \rightarrow J/\psi K^\pm$ channel used for calibration and performance estimation.



Flavour Tagging

Opposite Side Tagging Methods

Muon/electron tagging: semi-leptonic decay of B ($b \rightarrow \mu/e$ transition),

- flavour given by lepton charge,
- diluted by $b \rightarrow c \rightarrow \ell$ cascade decays and neutral B -meson oscillations,
- improved by using momentum weighed charge of lepton and tracks around the leading lepton

$$Q_\ell = \frac{\sum_i^{N_{\text{tracks}}} q_i p_{\text{T}i}^\kappa}{\sum_i^{N_{\text{tracks}}} p_{\text{T}i}^\kappa}, \quad (2)$$

where N_{tracks} is number of tracks in the cone $\Delta R < 0.5$ around the leading lepton, q_i and $p_{\text{T}i}$ are charge and p_{T} of the track, respectively, and the constant $\kappa = 1.1$ (found empirically).



b -jet-charge tagging: used if the additional muon/electron is absent; momentum-weighted track-charge in jet.

Flavour Tagging Calibration Curves

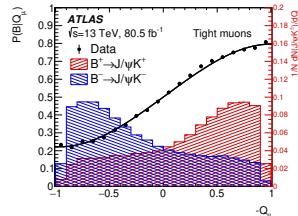
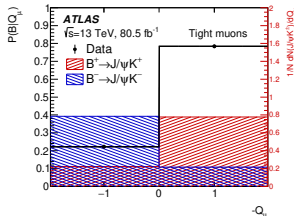
- From a calibration sample, the opposite-side charge is mapped to a probability that the meson is B_s^0 (or \overline{B}_s^0), and put into the likelihood fit on per-candidate basis.
- If there is no tagging information, $P = 0.5$ is assigned.

Tag method	Efficiency [%]	Effective Dilution [%]	Tagging Power [%]
Tight muon	4.50 ± 0.01	43.8 ± 0.2	0.862 ± 0.009
Electron	1.57 ± 0.01	41.8 ± 0.2	0.274 ± 0.004
Low- p_T muon	3.12 ± 0.01	29.9 ± 0.2	0.278 ± 0.006
Jet	12.04 ± 0.02	16.6 ± 0.1	0.334 ± 0.006
Total	21.23 ± 0.03	28.7 ± 0.1	1.75 ± 0.01

$$\epsilon_{\text{tag}} = \frac{N_{\text{tagged}}}{N_{\text{total}}}, \quad (3)$$

$$D_{\text{tag}} = 1 - \frac{2 N_{\text{wrong}}}{N_{\text{tagged}}}, \quad (4)$$

$$P_{\text{tag}} = \epsilon_{\text{tag}} \cdot D_{\text{tag}}^2. \quad (5)$$



Maximum Likelihood Fit Variables

- Observed variables (for i^{th} -candidate):
 - B_s^0 mass m_i and its uncertainty σ_{m_i} ,
 - B_s^0 proper decay time t_i and its uncertainty σ_{t_i} ; $t = \frac{L_{xy} m_B}{p_T}$,
 - 3 angles between final state particles in transversity basis $\Omega_i(\theta_{Ti}, \phi_{Ti}, \psi_{Ti})$ (see slide 6),
 - B_s^0 momentum p_{Ti} ,
 - B_s^0 tag probability $P(B|Q_i)$ and tagging method M_i .
- Determine 9 physics variables to describe $B_s^0 \rightarrow J/\psi\phi$ and S -wave:
 $\phi_s, \Delta\Gamma_s, \Gamma_s, |A_0(0)|^2, |A_{\parallel}(0)|^2, |A_S(0)|^2, \delta_{\parallel}, \delta_{\perp}, \delta_S$.

- Likelihood function:

$$\ln \mathcal{L} = \sum_{i=1}^N \left\{ w_i \cdot \ln \left(f_{\text{sig}} \cdot \mathcal{F}_{\text{sig}} + f_{\text{sig}} \cdot f_{B_d^0} \cdot \mathcal{F}_{B_d^0} + f_{\text{sig}} \cdot f_{\Lambda_b} \cdot \mathcal{F}_{\Lambda_b} + (1 - f_{\text{sig}}(1 + f_{B_d^0} + f_{\Lambda_b})) \cdot \mathcal{F}_{\text{bck}} \right) \right\}.$$

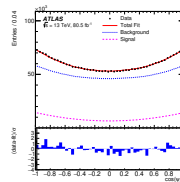
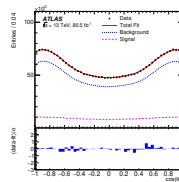
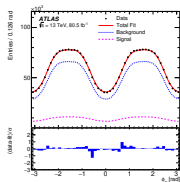
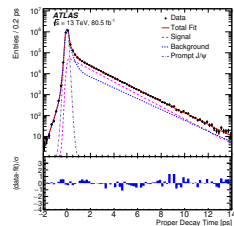
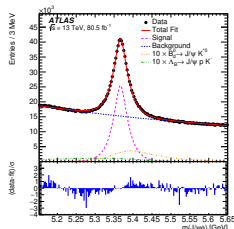


Fit Results

2015-2017 Data

- Fit projection to all data passing selections (2 977 526 B_s^0 candidates).
- Ratio plots include both stat. and syst. uncertainties; deviations within 2σ \Rightarrow total uncertainties cover any discrepancy between data and fit model.

Parameter	Value	Stat.	Syst.
ϕ_S [rad]	-0.081	0.041	0.020
$\Delta\Gamma_S$ [ps^{-1}]	0.0607	0.0047	0.0022
Γ_S [ps^{-1}]	0.6687	0.0015	0.0018
$ A_{\parallel}(0) ^2$	0.2213	0.0019	0.0022
$ A_0(0) ^2$	0.5131	0.0013	0.0034
$ A_S(0) ^2$	0.0321	0.0033	0.0044
$\delta_{\perp} - \delta_S$ [rad]	-0.25	0.05	0.04
δ_{\perp} [rad]	3.12	0.11	0.05
δ_{\parallel} [rad]	3.35	0.05	0.08



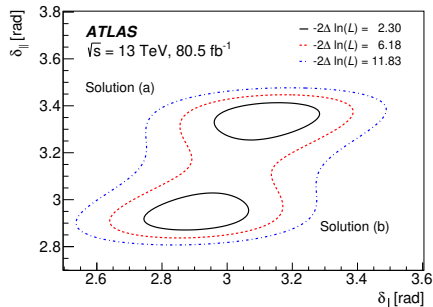
Fit to strong phases

2015-2017 Data

- Likelihood fit determined two solutions for the strong phases δ_{\parallel} and δ_{\perp} :
 - solution (a): $\delta_{\parallel} = 3.35$, $\delta_{\perp} = 3.12$ **vs.** solution (b): $\delta_{\parallel} = 2.94$, $\delta_{\perp} = 2.91$.
- Origin – an approximate symmetry in the signal PDF:

$$\{\delta_{\parallel}, \delta_{\perp}, \delta_S\} \rightarrow \{2(\pi - \delta_{\parallel}), \delta_{\perp} + (\pi - \delta_{\parallel}), \delta_{\perp} - \delta_S + (\pi - \delta_{\parallel})\}. \quad (6)$$

- – $2\Delta\ln(L)$ between the two solutions is to **0.03**, favouring (a) but without ruling out (b).
- Only a minor effect on all the variables.



Results

Combination Run1 + Data 2015-2017

- Ambiguity in sign of $\Delta\Gamma_s$:

$$\{\phi_s, \Delta\Gamma_s, \delta_\perp, \delta_\parallel\} \rightarrow \{\pi - \phi_s, -\Delta\Gamma_s, \pi - \delta_\perp, 2\pi - \delta_\parallel\}, \quad (7)$$

$\Delta\Gamma_s > 0$ constrained by LHCb [11].

- The combination makes use of a Best Linear Unbiased Estimate (BLUE) method [12, 13].
- Solutions (a) and (b) are almost identical (differences shown in red).

Parameter	Run1 Data			13 TeV Data			Combined		
	Value	Stat.	Syst.	Value	Stat.	Syst.	Value	Stat.	Syst.
ϕ_s [rad]	-0.090	0.078	0.041	-0.081	0.041	0.020	-0.087(8)	0.036	0.019
$\Delta\Gamma_s$ [ps^{-1}]	0.085	0.011	0.007	0.0607	0.0047	0.0022	0.0641(0)	0.0043	0.0024
Γ_s [ps^{-1}]	0.675	0.003	0.003	0.6687	0.0015	0.0018	0.6697(8)	0.0014	0.0015
$ A_\parallel(0) ^2$	0.227	0.004	0.006	0.2213	0.0019	0.0022	0.2221(18)	0.0017	0.0022
$ A_0(0) ^2$	0.522	0.003	0.007	0.5131	0.0013	0.0034	0.5149	0.0012	0.0031
$ A_S(0) ^2$	0.072	0.007	0.018	0.0321	0.0033	0.0044	0.0343(8)	0.0031	0.0044
$\delta_\perp - \delta_S$ [rad]	-0.08	0.03	0.01	-0.25	0.05	0.04	-0.24	0.05	0.04
δ_\perp [rad]	4.15	0.32	0.16	3.12	0.11	0.05	3.22	0.10	0.05
				2.91	0.11	0.05	3.03	0.10	0.05
δ_\parallel [rad]	3.15	0.10	0.05	3.35	0.05	0.08	3.36	0.05	0.08
				2.94	0.05	0.08	2.95	0.05	0.08



Results

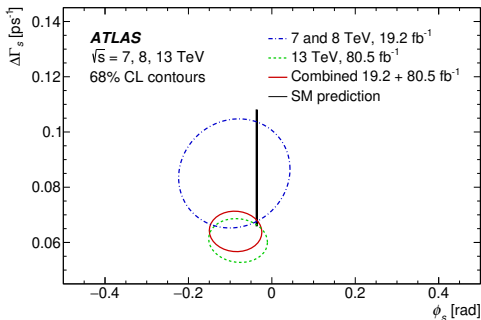
Combination Run1 + Data 2015-2017

- Ambiguity in sign of $\Delta\Gamma_s$:

$$\{\phi_s, \Delta\Gamma_s, \delta_\perp, \delta_\parallel\} \rightarrow \{\pi - \phi_s, -\Delta\Gamma_s, \pi - \delta_\perp, 2\pi - \delta_\parallel\}, \quad (7)$$

$\Delta\Gamma_s > 0$ constrained by LHCb [11].

- The combination makes use of a Best Linear Unbiased Estimate (BLUE) method [12, 13].
- Solutions (a) and (b) are almost identical.

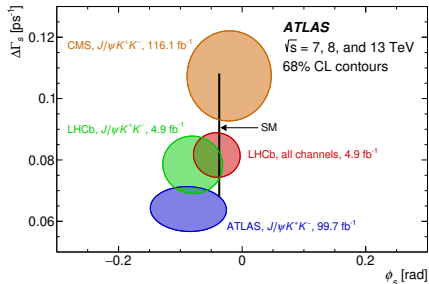
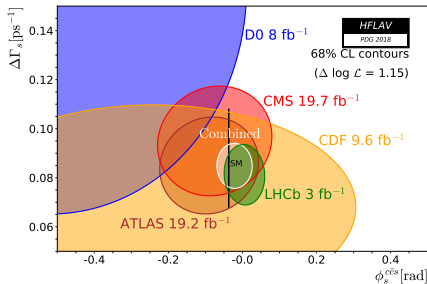


Comparison of the Results

(also Before vs. After)

	ϕ_s [rad]	$\Delta\Gamma_s$ [ps ⁻¹]	Comments, ref.
CMS	-0.021 ± 0.045	0.1073 ± 0.0097	[14]
LHCb	-0.081 ± 0.032	0.0777 ± 0.0062	$J/\psi K^+ K^-$, [15]
LHCb	-0.042 ± 0.025	0.0813 ± 0.0048	all channels, [15]
ATLAS	-0.087 ± 0.041	0.0641 ± 0.0049	[8]
SM	$-0.03696^{+0.00072}_{-0.00082}$	0.087 ± 0.021	[2], [17], resp.

- (Please note the different colour-code.)



Summary

- **ATLAS** has produced very **impressive** and **competitive** results.
- Analysis of the 2015+2016+2017 ATLAS data of 80.5 fb^{-1} performed.
- Results consistent with those obtained in the previous ATLAS analysis using 7 TeV and 8 TeV data, measurements statistically combined together.
- Compatible with the SM prediction.
- Our new measurement improves precision of the parameters.
- Analysis of full Run2 (60 fb^{-1} more) ongoing.
- **More public results on ATLAS B-physics TWiki page** <https://twiki.cern.ch/twiki/bin/view/AtlasPublic/BPhysPublicResults> !



THANK YOU!

BACKUP



Maximum Likelihood Fit

Probability Density Functions (PDF)

- Signal PDF consists of:
 - **mass PDF**: Gaussian with per-candidate width and scale-factor,
 - **time-angular PDF** convolved with time resolution function $G(t_i, \sigma_{t_i})$; flavour-dependent terms weighted by the corresponding tagging probability,
 - 4D angular **acceptance** (in bins of p_T , from MC),
 - empirical distributions of (conditional) observables σ_{m_i} , σ_{t_i} , p_{T_i} , and $P(B|Q)$
- Background PDF:
 - **mass PDF**: exponential + constant term,
 - **time PDF**: δ -function + 3 exponentials convolved with $G(t_i, \sigma_{t_i})$,
 - **angular PDF**: Legendre polynomial functions.

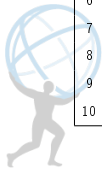


Decay Rate

- Ignoring detector effects, the distribution for the time and angles is given by the differential decay rate

$$\frac{d^4\Gamma}{dt d\Omega} = \sum_{k=1}^{10} \mathcal{O}^{(k)}(t) g^{(k)}(\theta_T, \psi_T, \phi_T). \quad (8)$$

k	$\mathcal{O}^{(k)}(t)$	$g^{(k)}(\theta_T, \psi_T, \phi_T)$
1	$\frac{1}{2} A_0(0) ^2 \left[(1 + \cos \phi_s) e^{-\Gamma_{\text{H}}^{(c)} t} + (1 - \cos \phi_s) e^{-\Gamma_{\text{H}}^{(b)} t} \pm 2e^{-\Gamma_{\text{H}} t} \sin(\Delta m_s t) \sin \phi_s \right]$	$2 \cos^2 \psi_T (1 - \sin^2 \theta_T \cos^2 \phi_T)$
2	$\frac{1}{2} A_{\parallel}(0) ^2 \left[(1 + \cos \phi_s) e^{-\Gamma_{\text{H}}^{(c)} t} + (1 - \cos \phi_s) e^{-\Gamma_{\text{H}}^{(b)} t} \pm 2e^{-\Gamma_{\text{H}} t} \sin(\Delta m_s t) \sin \phi_s \right]$	$\sin^2 \psi_T (1 - \sin^2 \theta_T \sin^2 \phi_T)$
3	$\frac{1}{2} A_{\perp}(0) ^2 \left[(1 - \cos \phi_s) e^{-\Gamma_{\text{H}}^{(c)} t} + (1 + \cos \phi_s) e^{-\Gamma_{\text{H}}^{(b)} t} \mp 2e^{-\Gamma_{\text{H}} t} \sin(\Delta m_s t) \sin \phi_s \right]$	$\sin^2 \psi_T \sin^2 \theta_T$
4	$\frac{1}{2} A_0(0) A_{\parallel}(0) \cos \delta_{\parallel} \left[(1 + \cos \phi_s) e^{-\Gamma_{\text{H}}^{(c)} t} + (1 - \cos \phi_s) e^{-\Gamma_{\text{H}}^{(b)} t} \pm 2e^{-\Gamma_{\text{H}} t} \sin(\Delta m_s t) \sin \phi_s \right]$	$\frac{1}{\sqrt{2}} \sin 2\psi_T \sin^2 \theta_T \sin 2\phi_T$
5	$ A_{\parallel}(0) A_{\perp}(0) \left[\frac{1}{2}(e^{-\Gamma_{\text{H}}^{(c)} t} - e^{-\Gamma_{\text{H}}^{(b)} t}) \cos(\delta_{\perp} - \delta_{\parallel}) \sin \phi_s \pm e^{-\Gamma_{\text{H}} t} (\sin(\delta_{\perp} - \delta_{\parallel}) \cos(\Delta m_s t) - \cos(\delta_{\perp} - \delta_{\parallel}) \cos \phi_s \sin(\Delta m_s t)) \right]$	$-\sin^2 \psi_T \sin 2\theta_T \sin \phi_T$
6	$ A_0(0) A_{\perp}(0) \left[\frac{1}{2}(e^{-\Gamma_{\text{H}}^{(c)} t} - e^{-\Gamma_{\text{H}}^{(b)} t}) \cos \delta_{\perp} \sin \phi_s \pm e^{-\Gamma_{\text{H}} t} (\sin \delta_{\perp} \cos(\Delta m_s t) - \cos \delta_{\perp} \cos \phi_s \sin(\Delta m_s t)) \right]$	$\frac{1}{\sqrt{2}} \sin 2\psi_T \sin 2\theta_T \cos \phi_T$
7	$\frac{1}{2} A_S(0) ^2 \left[(1 - \cos \phi_s) e^{-\Gamma_{\text{H}}^{(c)} t} + (1 + \cos \phi_s) e^{-\Gamma_{\text{H}}^{(b)} t} \mp 2e^{-\Gamma_{\text{H}} t} \sin(\Delta m_s t) \sin \phi_s \right]$	$\frac{2}{3} (1 - \sin^2 \theta_T \cos^2 \phi_T)$
8	$\alpha A_S(0) A_{\parallel}(0) \left[\frac{1}{2}(e^{-\Gamma_{\text{H}}^{(c)} t} - e^{-\Gamma_{\text{H}}^{(b)} t}) \sin(\delta_{\parallel} - \delta_S) \sin \phi_s \pm e^{-\Gamma_{\text{H}} t} (\cos(\delta_{\parallel} - \delta_S) \cos(\Delta m_s t) - \sin(\delta_{\parallel} - \delta_S) \cos \phi_s \sin(\Delta m_s t)) \right]$	$\frac{1}{3} \sqrt{6} \sin \psi_T \sin^2 \theta_T \sin 2\phi_T$
9	$\frac{1}{2} \alpha A_S(0) A_{\perp}(0) \sin(\delta_{\perp} - \delta_S) \left[(1 - \cos \phi_s) e^{-\Gamma_{\text{H}}^{(c)} t} + (1 + \cos \phi_s) e^{-\Gamma_{\text{H}}^{(b)} t} \mp 2e^{-\Gamma_{\text{H}} t} \sin(\Delta m_s t) \sin \phi_s \right]$	$\frac{1}{3} \sqrt{6} \sin \psi_T \sin 2\theta_T \cos \phi_T$
10	$\alpha A_0(0) A_S(0) \left[\frac{1}{2}(e^{-\Gamma_{\text{H}}^{(c)} t} - e^{-\Gamma_{\text{H}}^{(b)} t}) \sin \delta_S \sin \phi_s \pm e^{-\Gamma_{\text{H}} t} (\cos \delta_S \cos(\Delta m_s t) + \sin \delta_S \cos \phi_s \sin(\Delta m_s t)) \right]$	$\frac{4}{3} \sqrt{3} \cos \psi_T (1 - \sin^2 \theta_T \cos^2 \phi_T)$



Systematic Uncertainties

2015-2017 Data

	ϕ_s [10^{-3} rad]	$\Delta\Gamma_s$ [10^{-3} ps $^{-1}$]	Γ_s [10^{-3} ps $^{-1}$]	$ A_{ }(0) ^2$ [10^{-3}]	$ A_{\perp}(0) ^2$ [10^{-3}]	$ A_S(0) ^2$ [10^{-3}]	δ_{\perp} [10^{-3} rad]	$\delta_{ }$ [10^{-3} rad]	$\delta_{\perp} - \delta_S$ [10^{-3} rad]
Tagging	19	0.4	0.3	0.2	0.2	1.1	17	19	2.3
Acceptance	0.5	< 0.1	< 0.1	1.0	0.8	2.6	33	56	7.0
ID alignment	0.8	0.2	0.5	< 0.1	< 0.1	< 0.1	11	7.2	< 0.1
Best candidate selection	0.5	0.4	0.7	0.5	0.2	0.2	12	17	7.5
Background angles model:									
Choice of fit function	2.5	< 0.1	0.3	1.1	< 0.1	0.6	12	0.9	1.1
Choice of ρ_T bins	1.3	0.5	< 0.1	0.4	0.5	1.2	1.5	7.2	1.0
Choice of mass interval	0.4	0.1	0.1	0.3	0.3	1.3	4.4	7.4	2.3
Dedicated backgrounds:									
B_d^0	2.3	1.1	< 0.1	0.2	3.0	1.5	10	23	2.1
Λ_b	1.6	0.3	0.2	0.5	1.2	1.8	14	30	0.8
Alternate Δm_s	1.0	< 0.1	< 0.1	< 0.1	< 0.1	< 0.1	15	4.0	< 0.1
Fit model:									
Time res. sig frac	1.4	1.1	0.5	0.5	0.6	0.8	12	30	0.4
Time res. ρ_T bins	0.7	0.5	0.8	0.1	0.1	0.1	2.2	14	0.7
S-wave phase	0.3	< 0.1	< 0.1	< 0.1	< 0.1	0.2	8	15	37
Fit bias	5.7	1.3	1.2	1.3	0.4	1.1	3.3	19	0.3
Total	20	2.2	1.8	2.2	3.4	4.4	51	84	38



- Systematics assumed uncorrelated.
- Tagging systematics dominant for ϕ_s ; accounting for pile-up dependence, calibration curves model and MC precision, “Punzi” PDFs variations, difference between B^{\pm} and B_s^0 kinematics.
- Fit-model time resolution systematics dominant for Γ_s and $\Delta\Gamma_s$.

Correlation Tables

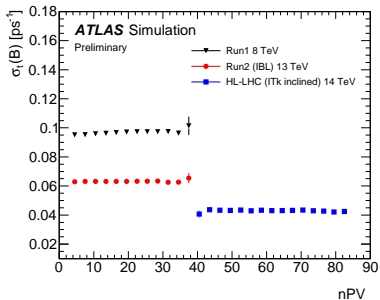
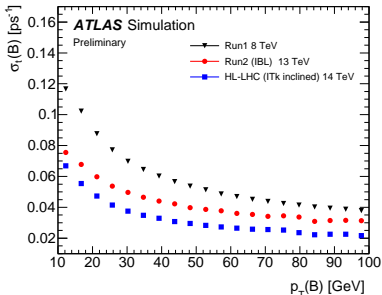
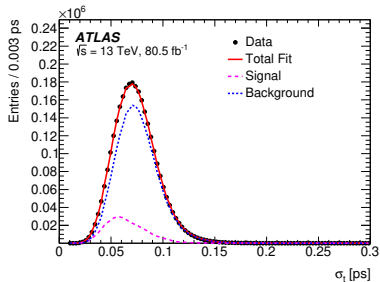
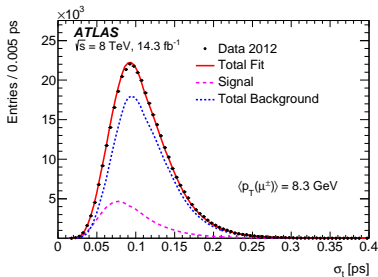
2015-2017 Data

	$\Delta\Gamma$	Γ_s	$ A_{ }(0) ^2$	$ A_0(0) ^2$	$ A_S(0) ^2$	$\delta_{ }$	δ_{\perp}	$\delta_{\perp} - \delta_S$
ϕ_s	-0.080	0.017	-0.003	-0.004	-0.007	0.007	0.004	-0.007
$\Delta\Gamma$	1	-0.586	0.090	0.095	0.051	0.032	0.005	0.020
Γ_s		1	-0.125	-0.045	0.080	-0.086	-0.023	0.015
$ A_{ }(0) ^2$			1	-0.341	-0.172	0.522	0.133	-0.052
$ A_0(0) ^2$				1	0.276	-0.103	-0.034	0.070
$ A_S(0) ^2$					1	-0.362	-0.118	0.244
$\delta_{ }$						1	0.254	-0.085
δ_{\perp}							1	0.001

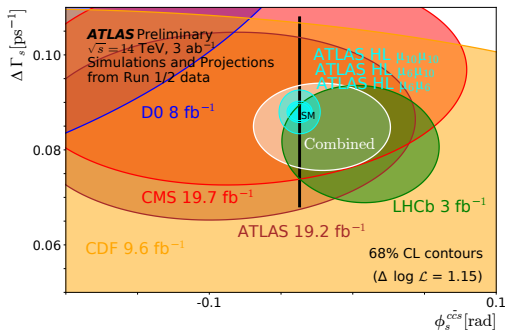
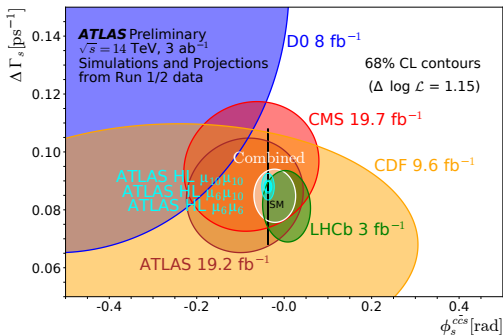
	$\Delta\Gamma$	Γ_s	$ A_{ }(0) ^2$	$ A_0(0) ^2$	$ A_S(0) ^2$	$\delta_{ }$	δ_{\perp}	$\delta_{\perp} - \delta_S$
ϕ_s	-0.084	0.019	-0.011	-0.003	-0.006	0.007	0.005	-0.006
$\Delta\Gamma$	1	-0.586	0.090	0.096	0.057	-0.029	-0.010	0.021
Γ_s		1	-0.116	-0.048	0.071	0.070	0.017	0.015
$ A_{ }(0) ^2$			1	-0.338	-0.110	-0.444	-0.106	-0.052
$ A_0(0) ^2$				1	0.269	0.080	0.017	0.070
$ A_S(0) ^2$					1	0.291	0.060	0.251
$\delta_{ }$						1	0.235	0.097
δ_{\perp}							1	0.056



Lifetime Uncertainty Plots (Run1, Run2, [19])



Prospects of CPV Measurements (Upgraded ATLAS, HL-LHC, [20])



CKM Matrix

Wolfenstein parametrization [21], [22]

$$V_{\text{CKM}} = \begin{pmatrix} 1 - \lambda^2/2 & \lambda & A\lambda^3(\rho - i\eta) \\ -\lambda & 1 - \lambda^2/2 & A\lambda^2 \\ A\lambda^3(1 - \rho - i\eta) & -A\lambda^2 & 1 \end{pmatrix} + \mathcal{O}(\lambda^4), \quad (9)$$

where the parameters A , ρ , and η are assumed to be of order one.



REFERENCES



References |

- [1] M. Kobayashi and T. Maskawa, *CP Violation in the Renormalizable Theory of Weak Interaction*, Prog. Theor. Phys. 49 (1973) 652.
- [2] J. Charles *et al.*, *Current status of the standard model CKM fit and constraints on $\Delta F = 2$ new physics*, Phys. Rev. D 91 (2015) no.7, 073007, numbers updated using the results from the 2019 values in https://ckmfitter.in2p3.fr/www/results/plots_summer19/ckm_res_summer19.html.
- [3] J. Pequeno, *Computer generated image of the whole ATLAS detector*, CERN-GE-0803012.
- [4] ATLAS Collaboration, *Invariant mass distributions for oppositely charged muon candidate pairs that pass various triggers, using 2018 data*, <https://twiki.cern.ch/twiki/bin/view/AtlasPublic/BPhysicsTriggerPublicResults>.
- [5] ATLAS Collaboration, *Time-dependent angular analysis of the decay $B_s^0 \rightarrow J/\psi\phi$ and extraction of $\Delta\Gamma_s$ and the CP-violating weak phase ϕ_s by ATLAS*, JHEP 1212 (2012) 072.
- [6] ATLAS Collaboration, *Flavor tagged time-dependent angular analysis of the $B_s \rightarrow J/\psi\phi$ decay and extraction of $\Delta\Gamma$ s and the weak phase ϕ_s in ATLAS*, Phys. Rev. D 90 (2014) no.5, 052007.
- [7] ATLAS Collaboration, *Measurement of the CP-violating phase ϕ_s and the B_s^0 meson decay width difference with $B_s^0 \rightarrow J/\psi\phi$ decays in ATLAS*, JHEP 1608 (2016) 147.
- [8] ATLAS Collaboration, *Measurement of the CP-violating phase ϕ_s in $B_s^0 \rightarrow J/\psi\phi$ decays in ATLAS at 13 TeV*, arXiv:2001.07115 [hep-ex].
- [9] CDF Collaboration, *Measurement of the CP-Violating Phase $\beta_s^{J/\psi\phi}$ in $B_s^0 \rightarrow J/\psi\phi$ Decays with the CDF II Detector*, Phys. Rev. D 85 (2012) 072002.
- [10]
- [11] LHCb Collaboration, *Determination of the sign of the decay width difference in the B_s system*, Phys. Rev. Lett. 108 (2012) 241801.



References II

- [12] R. Nisius, *On the combination of correlated estimates of a physics observable*, Eur. Phys. J. C 74 (2014) no.8, 3004.
- [13] R. Nisius, *BLUE: a software package to combine correlated estimates of physics observables within ROOT using the Best Linear Unbiased Estimate method - Program manual, Version 1.9.2*, <http://blue.hepforge.org>.
- [14] CMS Collaboration, *Measurement of the CP-violating phase ϕ_s in the $B_s^0 \rightarrow J/\psi \phi(1020) \rightarrow \mu^+ \mu^- K^+ K^-$ channel in proton-proton collisions at $\sqrt{s} = 13$ TeV*, arXiv:2007.02434 [hep-ex].
- [15] LHCb Collaboration, *Updated measurement of time-dependent CP-violating observables in $B_s^0 \rightarrow J/\psi K^+ K^-$ decays*, Eur. Phys. J. C 79 (2019) no.8, 706, Erratum: [Eur. Phys. J. C 80 (2020) no.7, 601].
- [16] F. Dordei, *Precision measurement of the CP-violating phase ϕ_s at LHCb*, LHC seminar, CERN, 7th May 2019, <https://indico.cern.ch/event/807907/>.
- [17] A. Lenz and U. Nierste, *Numerical Updates of Lifetimes and Mixing Parameters of B Mesons*, arXiv:1102.4274 [hep-ph].
- [18] Y. Amhis et al. (Heavy Flavour Averaging Group), *Averages of b-hadron, c-hadron, and τ -lepton properties as of summer 2016*, Eur. Phys. J. C 77 (2017) no.12, 895 and online update at <https://hflav.web.cern.ch>.
- [19] ATLAS Collaboration, *B_s^0 proper decay time resolution in the $B_s^0 \rightarrow J/\psi(\mu^+ \mu^-) \phi(K^+ K^-)$ decay for Run-1, Run-2 and HL-LHC*, <https://atlas.web.cern.ch/Atlas/GROUPS/PHYSICS/PLOTS/BPHYS-2016-001>.
- [20] ATLAS and CMS Collaborations, *Report on the Physics at the HL-LHC and Perspectives for the HE-LHC*, arXiv:1902.10229 [hep-ex].
- [21] L. Wolfenstein, *Parametrization of the Kobayashi-Maskawa Matrix*, Phys. Rev. Lett. 51 (1983) 1945.
- [22] A. J. Bevan et al., *The Physics of the B Factories*, Eur. Phys. J. C 74 (2014) 3026.

